Electronic Supplementary Information (ESI†)

Control of magnetic field distribution using nickel powder@PDMS pillars in microchannels

Xu Yu,[abc] Cong -Ying Wen,[ab] Zhi-Ling Zhang [ab*] and Dai-Wen Pang [ab]

[a]*Key Laboratory of Analytical Chemistry for Biology and Medicine (Ministry of Education), College of Chemistry and Molecular Sciences, and State Key Laboratory of Virology, Wuhan University, Wuhan, Hubei 430072, China;*

[b]*Wuhan Institute of Biotechnology, Wuhan, Hubei 430075, China;*

[c]*Department of Bioengineering, Pennsylvania State University, University Park, PA 16802, USA.*

*Correspondence: Professor Zhi-Ling Zhang; E-mail: zlzhang@whu.edu.cn;

Phone: +86-27-68756759; Fax: +86-27-68754067.

1. Culture of yeast cells

Yeast cells (S. Cerevisiae) were dipped from the broth with a bamboo stick and cultured in a solid plate. The yeast cells were cultured on the YPD solid plate containing 2% dextrose, 1% yeast extract, 2% peptone and 2% agar at 37 ºC, 2 d. While the yeast cells grew into a piece of colonies, a single colony was picked and transported into the yeast extract peptone dextrose medium (YPD, 2% dextrose, 1% yeast extract, 2% peptone). Then the yeast cells were cultured in the medium with a rotation of 200 rpm/min at 30 ºC for 24 h until they grew to the stable cycle. Before each experiment, 1% yeast was picked from the stable cycle and suspended in 5 mL fresh medium and at 30 ºC overnight with a rotation speed of 200 rpm. The yeast cells were centrifuged and re-suspended in the phosphate-buffered saline (1×PBS, pH 7.4) at the density of $1\times10^{6}\sim10^{7}$ cells/mL.

2. Conjugating Con A to the magnetic beads

The 1.05 μm magnetic beads with carboxyl groups were functionalized with Con A according to a two steps process. As Fig. 6(a) showed, 50 μL of 10 mg/mL magnetic beads were washed three times with MES buffer (50.0 mmol/L MES, 250.0 mmol/L NaCl, pH 6.0). Then, 50.0 mg/mL EDC and 50.0 mg/mL sulfo-NHS dissolved in cold MES buffer were added into the magnetic beads to activate the carboxyl groups for 30 min at room temperature. After that, the magnetic beads were washed once with the MES buffer and three times with 1.0×10^{-2} mol/L 1 × PBS (pH 7.4). After washing steps, 0.3 mg of Con A were added into the activated magnetic beads and dissolved in 1 × PBS to 250 μL. Then, the incubation step was completed in 4 hours with a slow tilt rotation of 120 rpm/min at room temperature. The Con A modified magnetic beads were washed three times by 600 μL of PBS-Tween 20 (0.05%, w/v) and once with 1 × PBS, then kept in 500 μL of 1 × PBS containing 1% BSA (w/v) and 0.05% NaN_3 (w/v) at 4 ºC.

3. Optical imaging of the nickel powder@pillar arrays

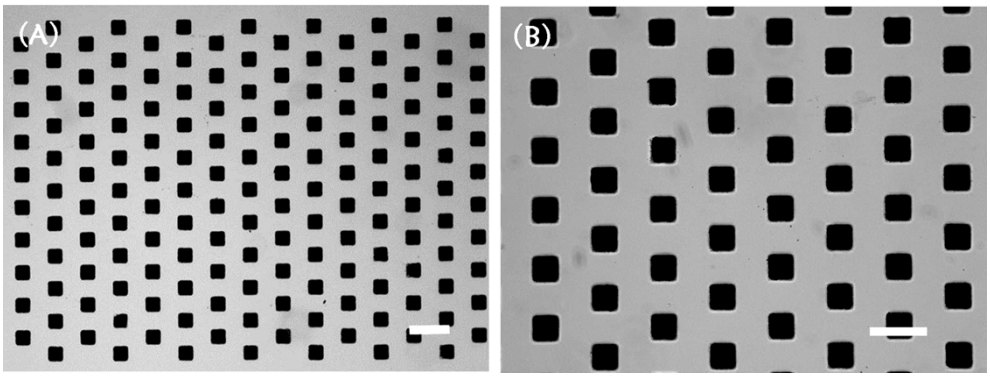

Fig. S1 Optical images of the nickel powder@PDMS pillars. (A) 90 μm nickel powder@PDMS pillars under the 4× object of an inverted fluorescence microscope. (B) The same nickel powder@PDMS pillars under 10× object of an inverted fluorescence microscope. The scale bars are 200 μm.

4. Simulation of the magnetic field distribution in the microchannels under the magnetic field-1 and magnetic field-2

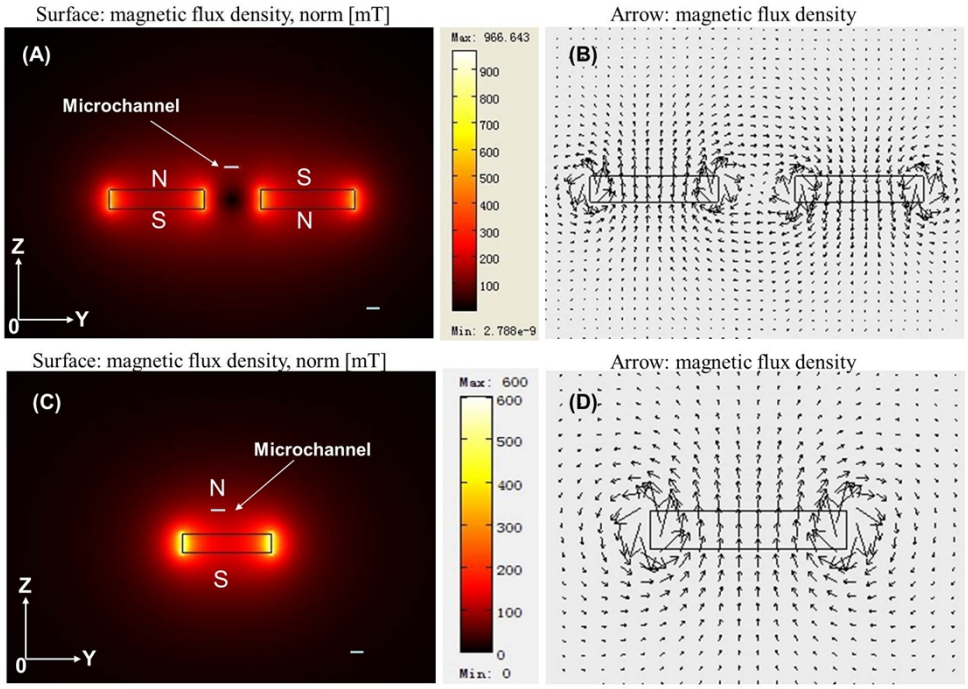

Fig. S2 The magnetic field distributions on two kinds of different external magnetic fields. (A) The magnetic field distribution on two magnets composed "NS" pole (magnetic field-1). (B) The arrow display of the magnetic flux density in A (YZ-plane). (C) The magnetic field distribution on one magnet (magnetic field-2). (D) The arrow display of the magnetic flux density in C (YZ-plane). The scale bars are 1 mm.

5. Numerical Simulation of the $|(B \cdot \nabla)B|$ Under the Magnetic Field-2

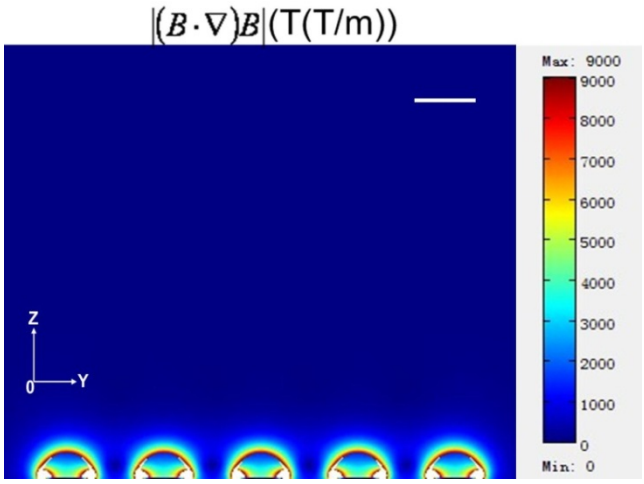

Fig. S3 Simulation of the $|(B \cdot \nabla)B|$ in the microchannel with the nickel powder@ PDMS pillars in the external magnetic field-2 (Z-axis direction, Z-Y plane). The scale bar is 50 μm.

6. Control of the Magnetic Field Distribution by Nickel Powder@PDMS Pillars

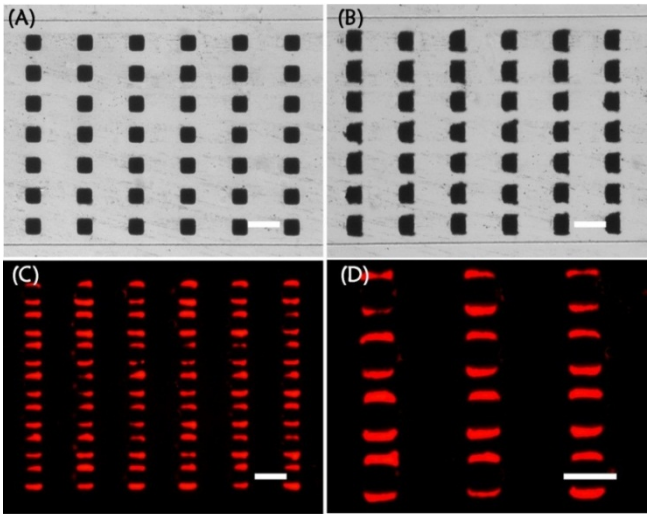

Fig. S4 Controlling the localized magnetic field distribution in the microchannel with general nickel powder@PDMS pillars. (A) Optical image of the nickel powder@PDMS pillars (50 μm × 50 μm). (B) Optical image of the captured fluorescent magnetic beads. (C) Fluorescence image of the captured red fluorescent magnetic nanoparticles under 10×object of an inverted fluorescence microscope. (D) Fluorescence image of the captured fluorescent magnetic nanoparticles under 20×object of an inverted fluorescence microscope. The scale bars are 100 μm.

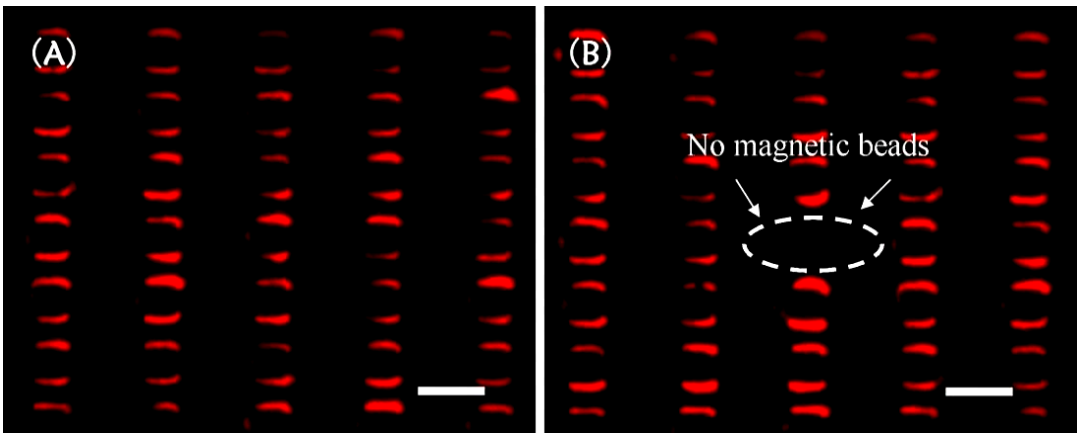

Fig. S5 (A) Fluorescence image of the captured red fluorescent magnetic nanoparticlls in a microfluidic chip with general nickel powder@PDMS pillars. (B) Fluorescence image of the captured fluorescent magnetic nanoparticles in a microfluidic chip with one defect unit of the nickel powder@PDMS pillars. The scale bars are 100 μm.

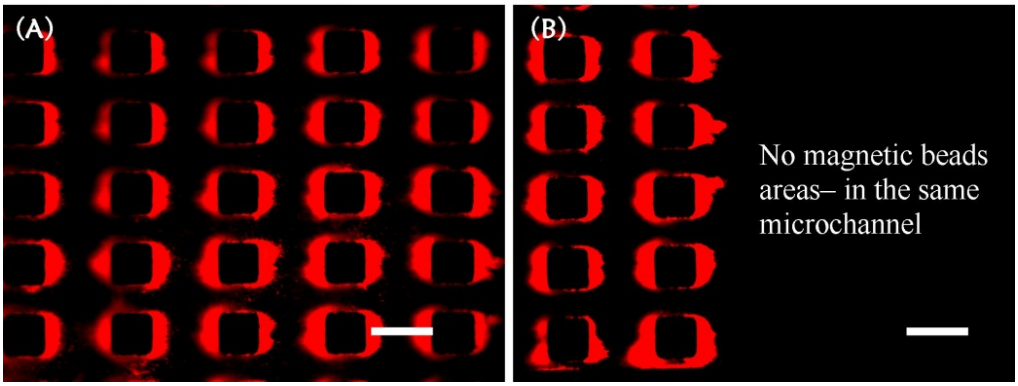

Fig. S6 Controlling the magnetic field distribution in the microchannel with nickel powder@PDMS pillars. (A) The red fluorescent magnetic nanoparticles captured under an upright external magnetic field. (B) No fluorescent magnetic nanoparticles being captured in the microfluidic channel where there was no nickel powder@PDMS pillar. The scale bars are 100 μm.